### Title
Species Concentration and Temperature Measurements in a Lean, Premixed Flow Stabilized by a Reverse Jet




### Journal
Combustion Science and Technology, 28(5-6)

### ISSN
0010-2202



### Authors
McDANNEL, MD
PETERSON, PR
SAMUELSEN, GS



### Publication Date
1982-08-01

### DOI
10.1080/00102208208952556

*Combustion Science and Technology*, 1982, Vol. 28, pp. 211–224
00010-2202/82/2805-0211$06.500


# Species Concentration and Temperature Measurements in a Lean, Premixed Flow Stabilized by a Reverse Jet

M. D. McDANNEL,† P. R. PETERSON‡ and G. S. SAMUELSEN§ *UCI Combustion Laboratory, Mechanical Engineering, University of California, Irvine, California 92717*

(*Received June 19, 1981; in final form December 15, 1981*)

**Abstract**—The chemical and thermal structure and the emission performance of an aerodynamic flameholder are presented and examined. Recirculation is established by injecting a premixed jet into an opposing mainstream of premixed reactants. The injection of the jet directly into the recirculation zone provides a control of the stabilization zone mixture ratio, temperature, and size not found in bluffbody flameholding. The size and stoichiometry of the recirculation zone is dictated by the jet velocity and mixture ratio respectively. A parametric study of the controlling variables (main and jet stream velocities, main and jet stream equivalence ratios) reveals the partitioning between the recirculation zone and wake in both the heat release and pollutant production. An examination of the emission indexes and flowfield profiles of temperature and species concentration establishes the influence and control of jet and mainstream conditions on pollutant production. A reduction in jet velocity and/or an enrichment of the jet, for example, effects a substantial change in $NO_x$ emission. Further, jet enrichment extends the lean blow-off limit of the mainstream. There exists a point, however, beyond which the reaction is not supported in the wake and further leaning of the mainstream results in a substantial emission of unspent fuel.

## INTRODUCTION

The present demand to develop energy-efficient and low-emission combustion systems requires tailoring the combustor aerodynamics to more effectively control the temperature field, the distribution of fuel, and the limits of flame stability. Aerodynamic flameholding offers some advantages in this regard as an alternative to conventional bluffbody or sudden expansion flameholding.

A reverse jet flameholder is shown in Figure 1. The incoming mainstream of premixed fuel and air is opposed by a high velocity jet positioned along the longitudinal axis. The jet creates the zone of recirculating flow necessary to stabilize the reaction. The jet stream, also composed of premixed fuel and air, constitutes a few percent of the total flow entering the combustor, but contributes as much as one third to the mass within the recirculation zone. As a result, a wide range of stable combustion conditions may be achieved by independently varying the mixture ratios and velocities of the jet and maintstream (Figure 2). Most notably, by enriching the jet, the lean blow-off limit can be significantly extended.

The reverse jet ("opposed jet") flameholder was first introduced as a candidate for flameholding in afterburners (Schaffer, 1954). Jets injected at an angle from the wall, were proposed for stabilizing the reaction during afterburner operation while avoiding the attendant pressure drop associated with conventional, physical flameholders when afterburning was not in use. Adoption proved to be infeasible, however, upon the discovery that the flameholding performance of the reverse jet drops sharply when the jet is located at small angles (*ca.* 5°) to the opposing flow (Duclos *et al.*, 1957).

The reverse jet has been used more recently as a vehicle to test elliptic codes for both reacting (*e.g.* Peck and Samuelsen, 1977; Schefer and Sawyer, 1977), heated (*e.g.* Elghobashi *et al.*, 1981), and cold (*e.g.* Wuerer and Samuelsen, 1979) flows. It has the advantage of separating the recirculation

†Present address: KVB Engineering, Inc., P.O. 19518, Irvine, CA 92714.

‡Present address: Pacific Environmental Services, 1905 Chapel Hill Road, Durham, NC 27707.

§To whom correspondence should be addressed: Mechanical Engineering, University of California, Irvine, CA 92717.

(a) Schematic

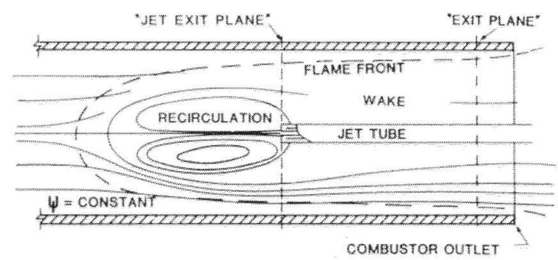


(b) Predicted velocity vectors (Peck and Samuelsen, 1977)

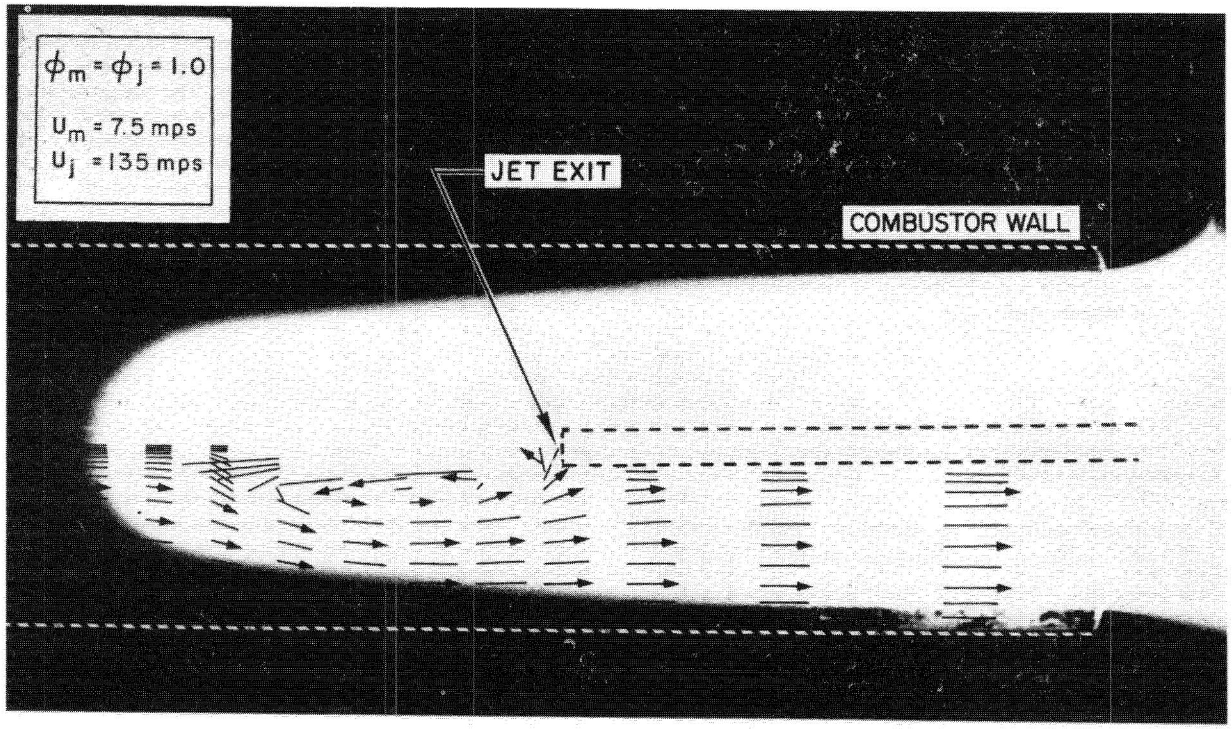


FIGURE 1 Reverse jet flameholder.

zone from solid boundaries, and promoting major changes in the extent of reaction by small perturbations in the condition of the reverse jet.

Practical applications now include the use of the reverse jet as an ignition source in catalytic combustion (Anderson *et al.*, 1981). The jet flameholder (Figure 3) stabilizes the premixed reactants upstream of the catalyst, and the products of combustion serve as the energy source for catalytic heat-up. Once the catalyst is active, the jet-supported flame is extinguished by terminating flow to the jet while keeping to a minimum the residual pressure drop associated with the jet tube.

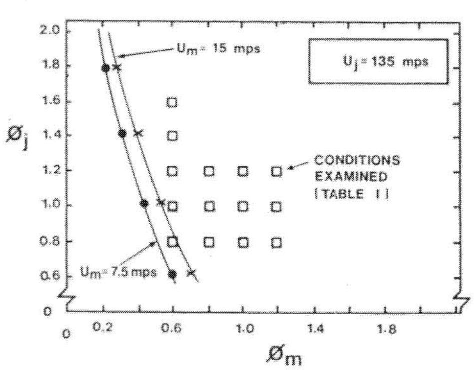


FIGURE 2 Lean extinction limit for propane-air.

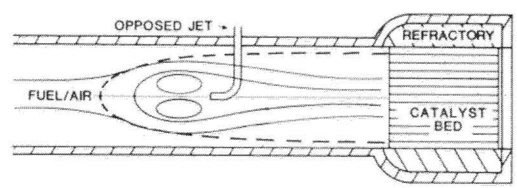


FIGURE 3 Catalytic combustor with reverse jet ignition

The objective of the present study is to provide a general characterization of the chemical and flame structure for a range of parametric variations of the four primary controlling variables: Main and jet stream equivalence ratios, main and jet stream velocities. Exit plane and detailed flowfield profiles are presented and analyzed for $NO_x$, carbon monoxide (CO), total hydrocarbons (HC), and temperature. The goals are to provide (1) insight into the performance of a reverse jet, aerodynamic flameholder, (2) guidance for practical applications of aerodynamic flameholding, and (3) a data base for future code testing.

## EXPERIMENT

### *Combustor*

The experimental facility is shown in schematic in Figure 4. The combustor consisted of a 51 mm (2-inch) i.d. quartz cylindrical chamber with an overall length of 457 mm (18-inches). The jet stream issued from a 1.32 mm (0.052-inch) i.d. hole at the end of a 6.35 mm (0.25-inch) o.d., water-cooled, stainless steel jet tube. The jet tube exit was located upstream of the combustor outlet. Combustion air was supplied by the building compressed air system and was dried and filtered prior to introduction to the combustor. Commercial grade propane was supplied from pressurized cylinders. A complete description of the test facility and test analysis system is available (Peterson and Himes, 1978).

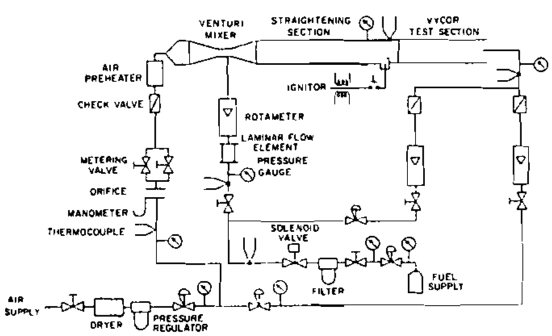


FIGURE 4 Schematic of combustor facility.

### *Species and Temperature Measurements*

Temperatures were measured using an unshielded, fine wire, platinum/platinum-13 percent rhodium thermocouple mounted on a micrometer traverse jig. A Doric digital pyrometer (Model DS-500) was used to record the thermocouple output. The values for temperature reported are uncorrected for radiation.

Combustion gases were sampled continuously using a hot (60°C/140°F) watercooled, 6.35 mm (0.25-inch) o.d. by 1.32 mm (0.052-inch) i.d., stainless probe with a constant area inlet bounded by a cooled, streamlined tip. The sample probe was mounted on a micrometer traverse jig for sampling. The gas sample flowed to the analysis instruments through heated (65°C/150°F), 6.35 mm (0.25-inch) o.d. Teflon tubing.

For detailed flowfield maps, radial traverses were taken at twelve axial locations, with the distance between axial locations ranging from 2.54 mm (0.1-inch) in the nose of the recirculation zone to up to 24.13 mm (0.95-inch) between the jet tube exit and combustor "exit plane" (a plane arbitrarily located 13 mm upstream of the combustor outlet and 67 mm downstream of the jet tube exit). Radial locations were at 3.05 mm (0.12-inch) increments between the jet tube wall and the chamber wall.

Analysis of the sample gas was performed using a packaged emission analysis system (Scott Research, Model 113). Passage of the gas through an ice bath allowed all concentration measurements to be taken on a dry basis. Nitrogen oxides (NO, $NO_x$) concentrations were measured using a chemiluminescence analyzer (Scott Research, Model 125). Nondispersive infrared analyzers (Beckman, Models 315B and 315BL respectively) were used to measure carbon dioxide ($CO_2$) and carbon monoxide (CO) concentrations. Total hydrocarbon (HC) concentration was measured by a flame ionization detector (Scott Research, Model 215). Oxygen ($O_2$) concentration was measured by a paramagnetic analyzer (Scott Research, Model 150).

### *Test Conditions*

The test conditions are tabulated in Table I. The following conditions represented the BASE CASE:

- Main Stream Reference Velocity $U_m = 7.5$ m/s
- Jet Stream Reference Velocity $U_j = 135$ m/s
- Main Stream Equivalence Ratio $\phi_m = 1.0$
- Jet Stream Equivalence Ratio $\phi_j = 1.0$

Results are presented first for the BASE CASE. Second, parametric variations are presented in the order listed in Table I. Each of the four controlling variables ($\phi_m$, $\phi_j$, $U_j$, $U_m$) were evaluated. Note

TABLE I
Test conditions

| $U_m$ (mps) | $U_j$ (mps) | $\phi_m$ | $\phi_j$ | Parametric variation |
|---|---|---|---|---|
| 7.5 | 135 | 1.0 | 1.0 | BASE CASE |
| 7.5 | 135 | 1.2 | 0.8, 1.0, 1.2 | |
| | | 1.0 | 0.8, 1.0, 1.2 | $\phi_m$, $\phi_j$ |
| | | 0.8 | 0.8, 1.0, 1.2 | |
| | | 0.6 | 0.8, 1.0, 1.2, 1.4, 1.6 | |
| 7.5 | 70 | 1.0 | 1.0 | $U_j$ |
| 15.0 | 135 | 1.0 | 1.0 | $U_m$ |

(Table I) that the mainstream equivalence ratios ($\phi_m$) were biased to fuel lean mixture ratios because of the interest in lean mainstream emission performance. The jet equivalence ratios ($\phi_j$) were biased to the fuel rich mixture ratios to extend the lean limit of the main stream mixture. The range of main stream ($U_m$) and jet velocities ($U_j$) allowed an examination of the effects of recirculation zone size and stoichiometry on flame structure and pollutant emission.

Finally, emission indexes are presented to summarize the emission behavior of the combustor at the conditions considered, and to provide a practical perspective to the utility of opposed jet flameholding. A complete set of the data and results is available (McDannel, 1979).

## RESULTS AND DISCUSSION

### A. *Base Case*

The detailed flowfield maps and exit plane profiles for the base case are presented in Figure 5. Two distinct regions can be deduced from the results (Figure 6). One is the *recirculation zone*, which is a zone of strong backmixing driven by the jet flow. The other is a radially propagating reaction in the *wake* of the recirculation zone. For example, the oxidation of hydrocarbons (Figure 5a) and formation of carbon monoxide (CO) occurs within the recirculation zone where there is intense mixing of reactants with hot products, and along the radially propagating wake reaction front. Within the wake, temperature, oxygen, and residence time are sufficient to ensure nearly complete HC consumption, and to initiate the oxidation of CO to carbon dioxide ($CO_2$) as demonstrated by the decrease in CO concentration adjacent to the jet tube proceeding downstream toward the exit plane. Proceeding toward the combustor wall, the concentrations of HC and $O_2$ approach those of the reactants. As a result, the source of the hydrocarbons emitted at the exit plane is the area outside of the wake.

Oxides of nitrogen ($NO_x$) are formed thermally in both the recirculation zone and wake as a result of elevated temperatures, sufficient residence time, and available oxygen. Area-averaged concentrations calculated at both the "jet exit plane" and combustor "exit plane" (Figure 1a), indicate that 75 percent of the total $NO_x$ emitted is formed in the recirculation zone for this base condition.

The exit plane profiles (Figure 5b) show the general structure of the wake. Within the wake and proceeding from the jet tube to the combustor wall, HC and oxygen concentrations and temperature remain relatively constant, while CO concentrations increase slowly and $NO_x$ concentrations decrease. At approximately $r/R = 0.55$, the concentrations of HC, $CO_2$, and $O_2$ change sharply. Oxygen and HC rise, $CO_2$ drops and CO peaks. Eventually, the HC and $O_2$ rise to the reactant concentrations.

Finally, it is noteworthy that the $NO/NO_x$ ratio drops abruptly at the flame front (Figure 5b). This is attributed to the rapid mixing of hot products and cold reactants at the flame front which produce radical relaxation reactions and associated populations of hydroperoxy radicals ($HO_2$) sufficient to oxidize NO to $NO_2$. Unfortunately, these events can be influenced by the probe, and the extent to which the measured levels of $NO_2$ are real or artifacts of the probe remains unanswered. However, an evaluation (Chen, *et al.*, 1979) of similar observations in a premixed combustor (Oven, *et al.*, 1979) concluded that, although measurements within high temperature reaction zones (*e.g.*, within the recirculation zone and wake) are likely biased by probe-induced oxidation of NO, elevated levels of $NO_2$ in areas of rapid flame quench (*e.g.*, the flame front) are likely real and not artifacts of the probe.

(a) Flow maps.

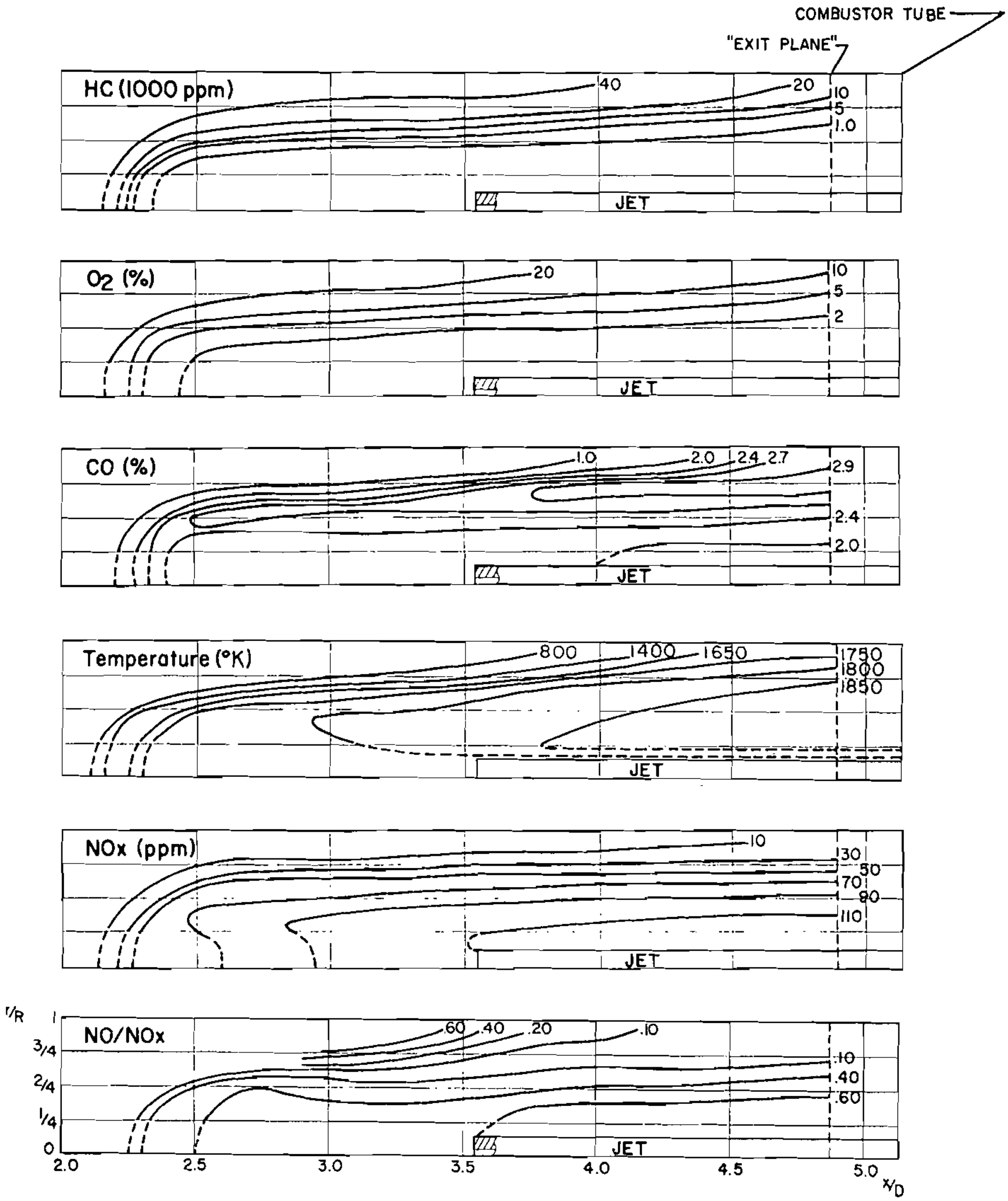


FIGURE 5 Base case.

(b) Exit plane profiles.

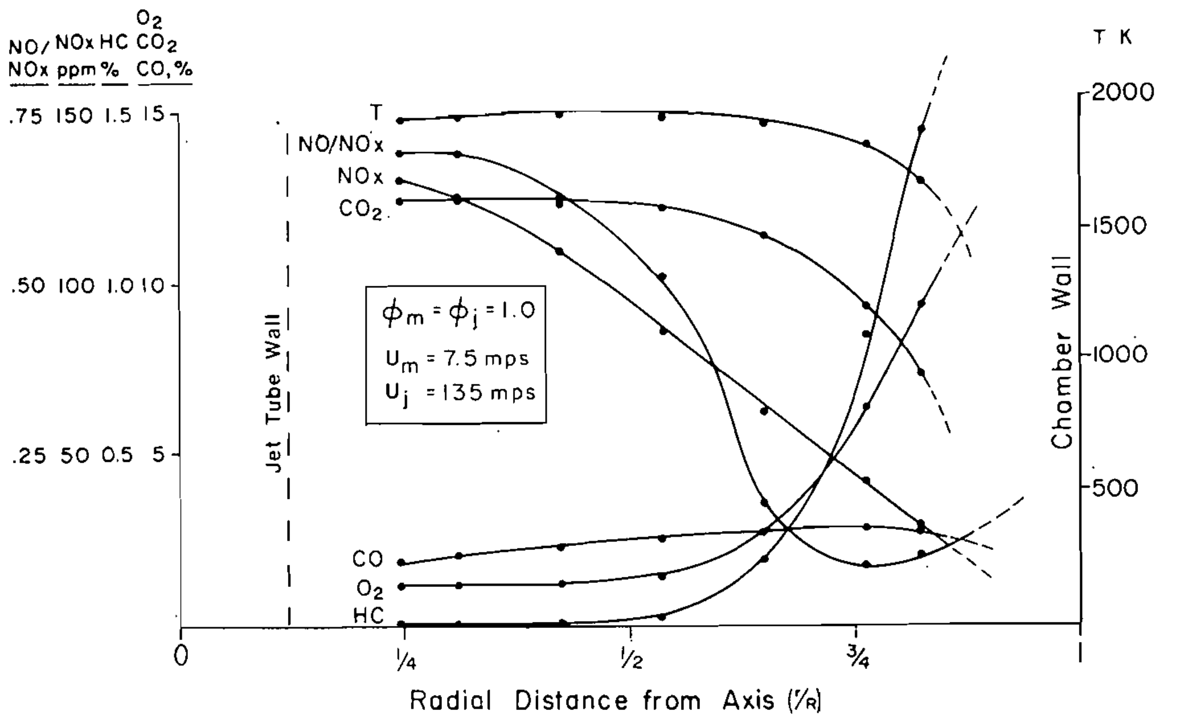


FIGURE 5 Base case (concluded).

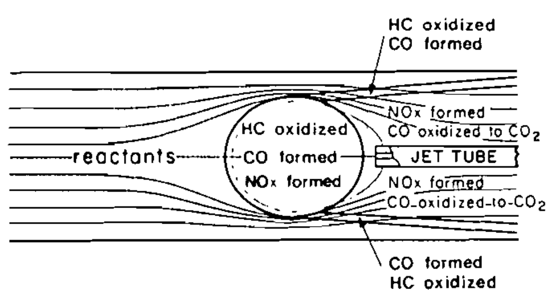


FIGURE 6 Heat release and pollutant formation scenario.

B. *Parametric Study*

*Mainstream and Jet Velocities*

The major effect of changing mainstream and jet velocity is to change the size of the recirculation and wake region. This is demonstrated in the present study by independently increasing the mainstream velocity ($U_m$) and decreasing the jet velocity ($U_j$). The effect of either is to decrease the size of the recirculation and wake regions.

The visual appearance of the flame for the base case and two variations on the base case is shown in Figure 7. Both the penetration of the jet and the radial propagation in the wake are restricted by increasing the mainstream velocity or by decreasing the jet velocity. This is confirmed by the detailed temperature maps presented in Figure 8.

A decrease in the size of the recirculation and wake reaction zones produce a net reduction in residence time and, hence, a net reduction in the $NO_x$ production (Figure 9).

*Mainstream and Jet Equivalence Ratios*

The mainstream equivalence ratio ($\phi_m$) is the dominant variable controlling the heat release and, ultimately, the pollutant emission. The effect on heat release is shown in Figure 10.

*HC, CO, T.* As indicated by HC exit plane profiles, the wake reaction propagates further radially as the mainstream mixture is enriched. This is a consequence of the decrease in air dilution as $\phi_m$ is increased from 0.6 to 1.0. The increase in wake reaction as $\phi_m$ is enriched from 1.0 to 1.2 is attributed to an increased availability of hydrocarbon radicals. Peak flame velocities for propane-air flames generally occur at equivalence ratios rich of stoichiometric (Fristrom and Westenberg, 1965).

(a) Base case

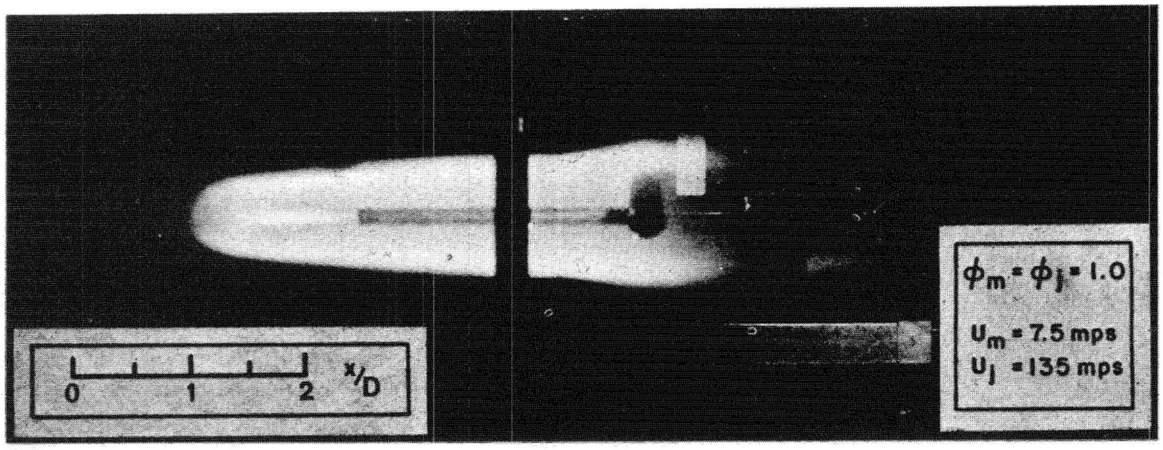


(b) Elevated mainstream velocity ($U_m$)

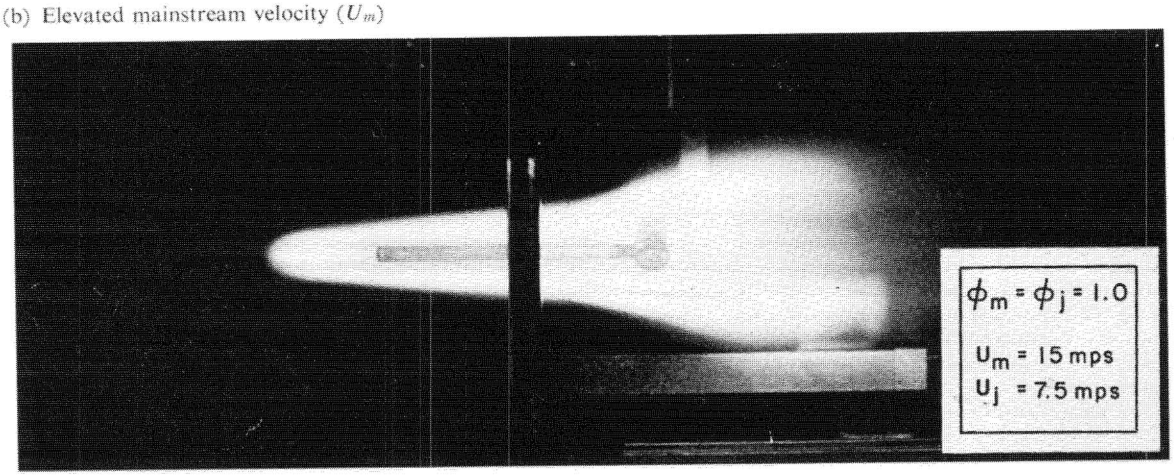


(c) Reduced jet velocity ($U_j$)

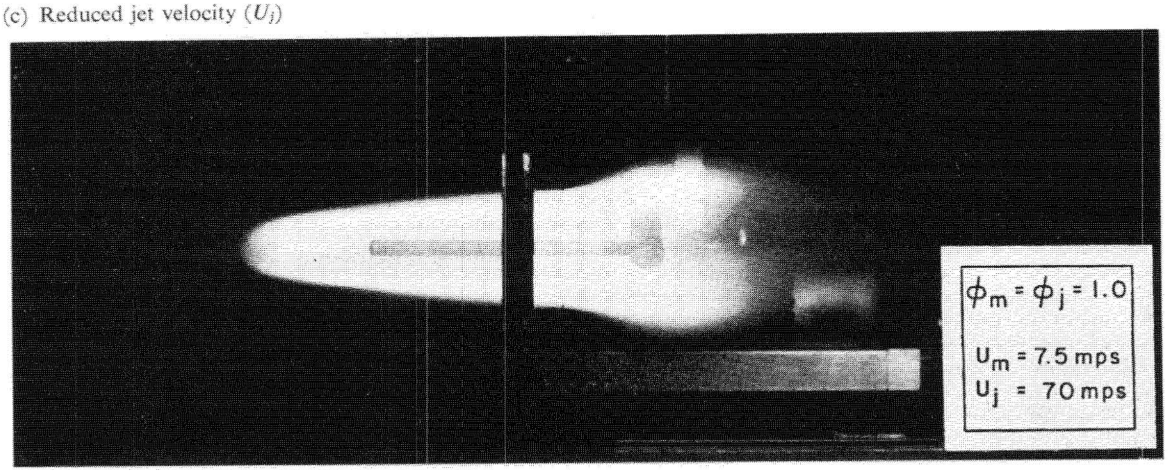


FIGURE 7 Parametric study: Effect of $U_m$ and $U_j$ (flame shape).

(a) Temperature exit plane profile

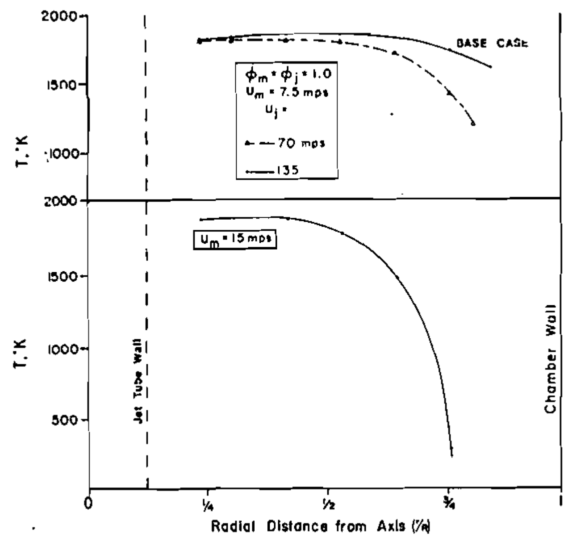


The highest temperatures occur for the base case ($\phi_m = 1.0$). Peak temperatures are about 300°K lower for $\phi_m = 1.2$ and 500°K lower for 0.8.

Carbon monoxide concentrations increase with mainstream equivalence ratio as the amount of available oxygen to oxidize CO to $CO_2$ decreases. For all conditions, the temperature is sufficient for the oxidation to occur. For equivalence ratios of 0.8 to 1.0, peak concentrations correspond to the location of the wake reaction front. Inside the front, CO is oxidized to $CO_2$. This accounts for the increase in temperature in the wake. Ahead of the front, CO diffuses into the cold reactant gases.

At $\phi_m = 1.2$, the absence of oxygen in the wake results in relatively constant CO concentrations and an absence of a distinct CO peak at the flame front.

For all cases except $\phi_m = 0.6$, temperatures are fairly constant within the wake reaction zone and

(b) Temperature flow maps.

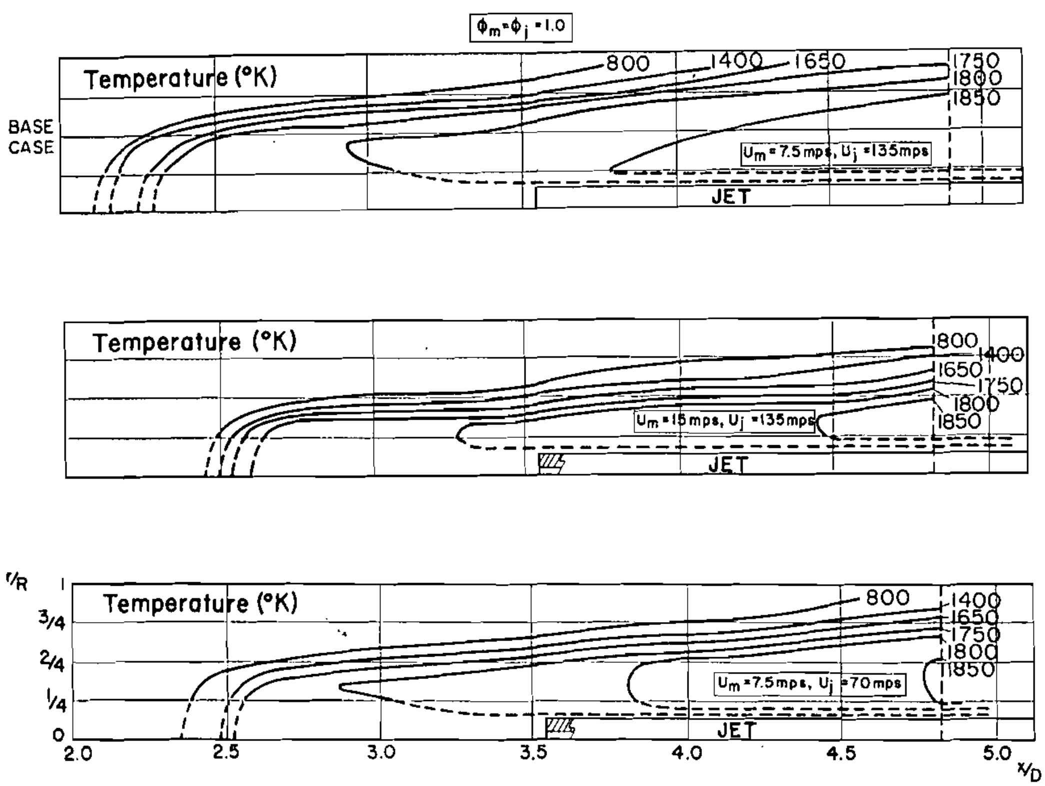


FIGURE 8 Parametric study: Effect of $U_m$ and $U_j$ ($T$).

(a) $NO_x$ exit plane profiles

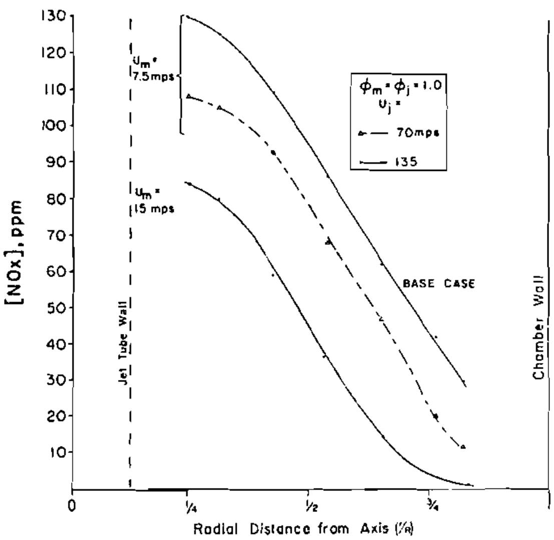


drop at the radially propagating wake reaction front. For $\phi_m=0.6$, the temperatures drop immediately adjacent to the axis, and HC concentrations remain elevated while CO concentrations fall instead of rise when proceeding from the axis to the chamber wall. This suggests that reaction in the wake is suppressed and CO formation, for example, is restricted to the recirculation region upstream with radial diffusion in the wake. Note that CO concentrations for $\phi_m=0.6$ are not appreciably lower than for $\phi_m=0.8$. In fact, near the jet tube, concentrations are lower for $\phi_m=0.8$. The additional oxygen available at $\phi_m=0.6$ is offset by lower temperatures.

Varying the jet stream equivalence ratio ($\phi_j$) allows determination of the effect of recirculation zone mixture ratio. The effect on exit plane profiles of HC and temperature is pronounced only at $\phi_m=$ 0.6. Higher jet equivalence ratios result in lower HC concentrations near the jet tube wall and higher

(b) $NO_x$ flow maps.

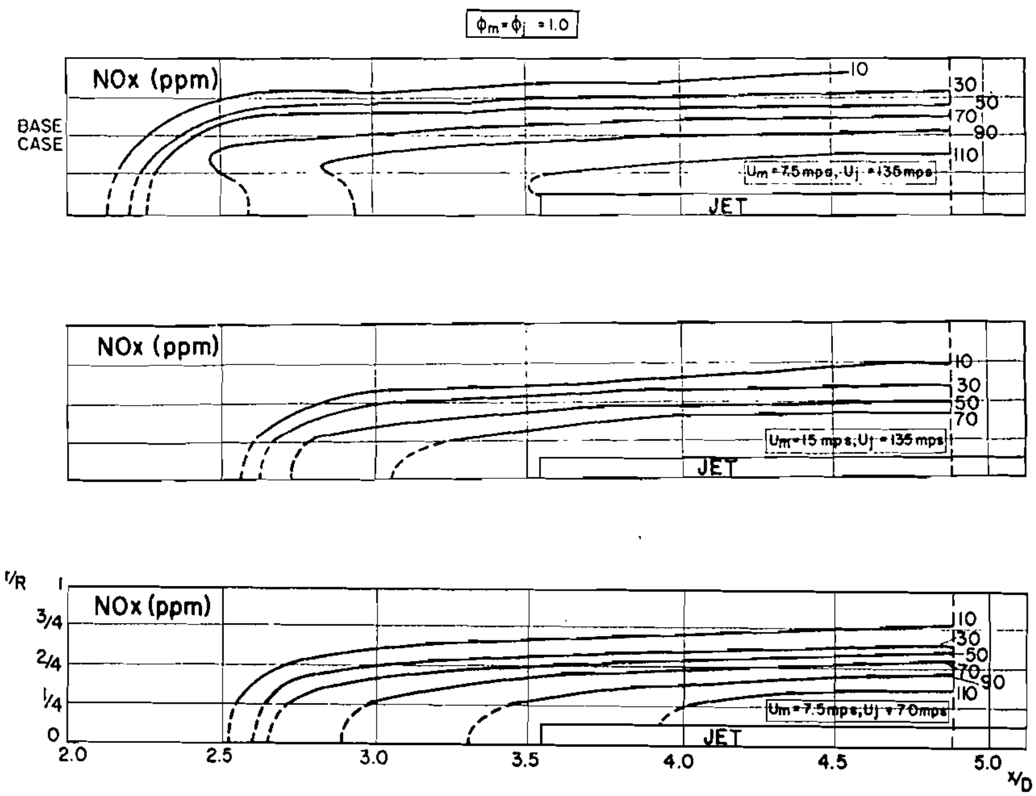


FIGURE 9 Parametric study: Effect of $U_m$ and $U_j$ ($NO_x$).

temperatures, and this effect diminishes as distance from the jet tube wall increases. This is attributed to higher temperatures in the recirculation zone that result from recirculation zone mixture ratios closer to stoichiometric. This effect is not as pronounced for the other equivalence ratios because each effectively sustains a fully developed reaction in the wake.

The effect of jet equivalence ratio on carbon monoxide is noticeable only near the jet tube. For $\phi_m = 0.6$, richer jet mixtures result in lower CO emissions because of higher temperatures in combination with the elevated concentration of oxygen. This same trend occurs, but to a much lesser extent, for $\phi_m = 0.8$. At $\phi_m = 1.0$ and 1.2 this trend is reversed. For these cases oxygen, and not temperature, limits the CO oxidation.

(a) HC exit plane profiles

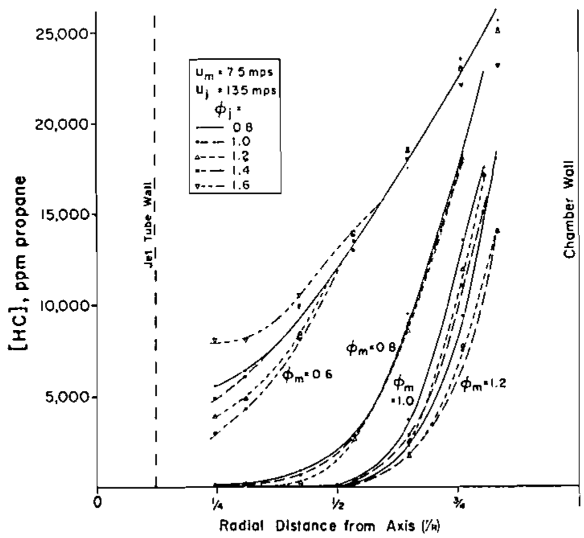


(b) CO exit plane profiles

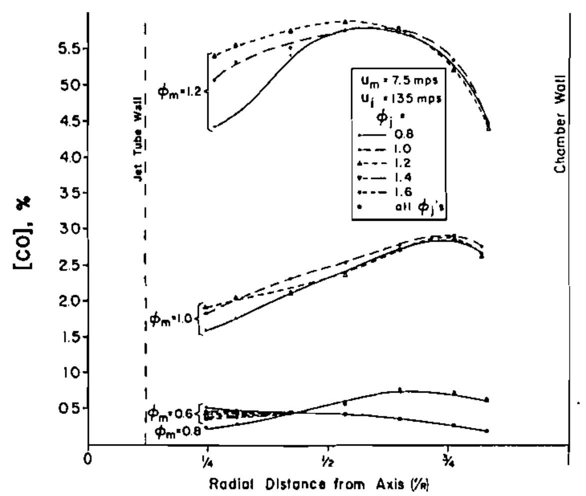


c) Temperature exit plane profiles

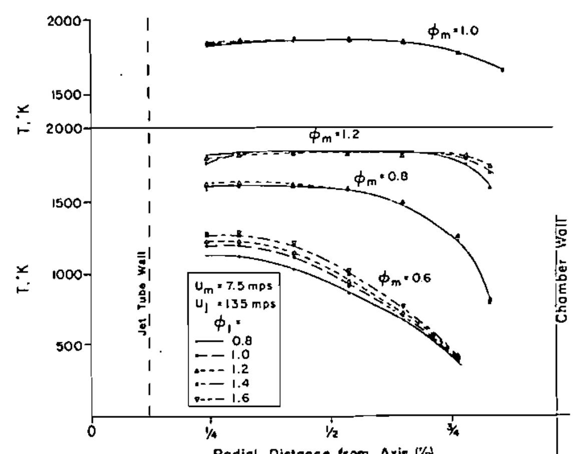


FIGURE 10

(d) Temperature flow maps.

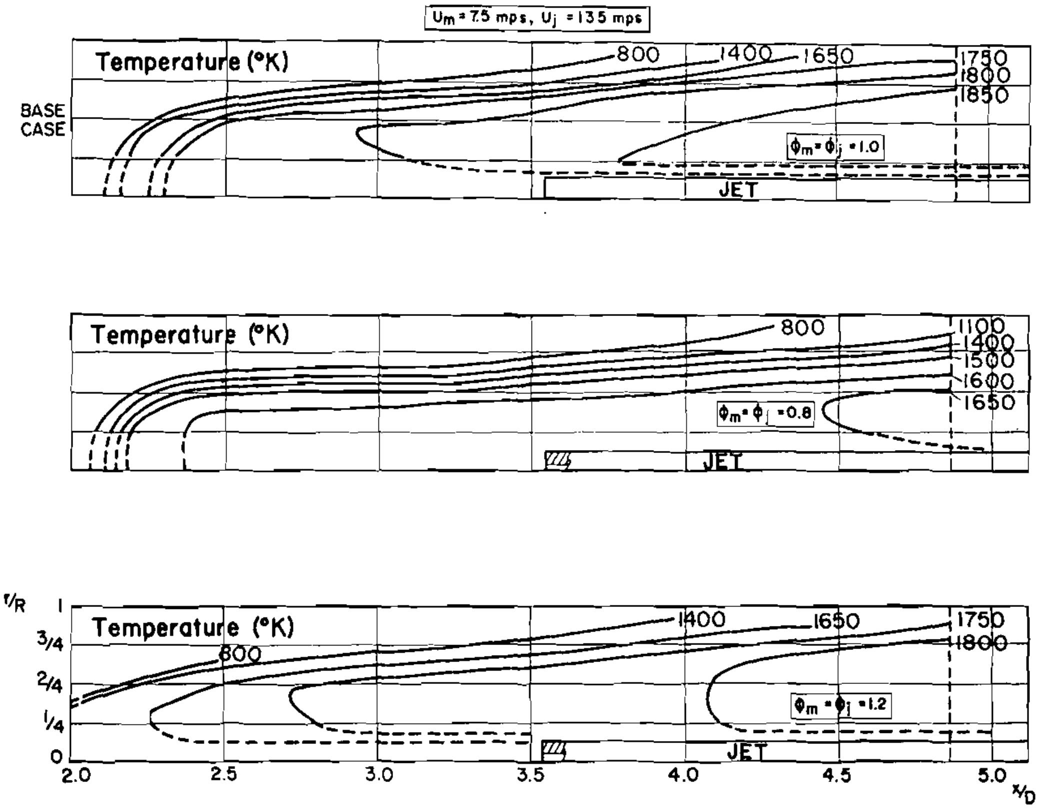


FIGURE 10 Parametric study: Effect of $\phi_m$ and $\phi_j$ (HC, CO, T).

(a) $NO_x$ exit plane profiles.

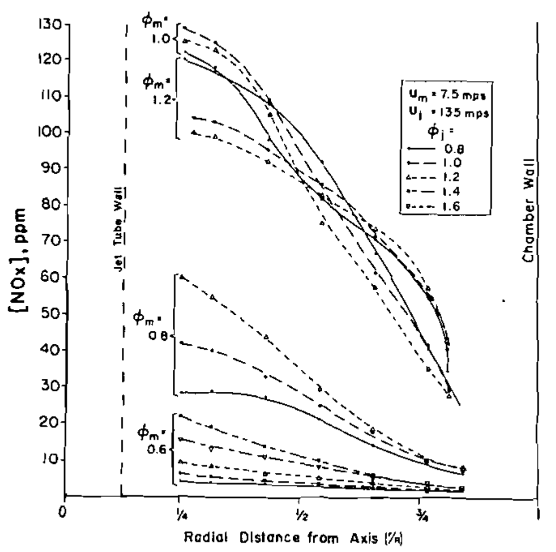


FIGURE 11 Parametric study: Effect of $\phi_m$ and $\phi_j$ ($NO_x$)

*$NO_x$.* The $NO_x$ profiles are presented in Figure 11. Peak concentrations are highest for the base case ($\phi_m = 1.0$). The concentrations are slightly lower at $\phi_m = 1.2$. For the leaner cases, there is a significant drop in concentrations.

For all cases the shape of the $NO_x$ exit plane profile is similar, decreasing almost linearly from the jet to the combustor wall. The shape indicates that most of the $NO_x$ is formed in the recirculation zone, and diffuses by turbulent transport downstream. This is confirmed in the detailed flow maps presented in Figure 11b. These trends correspond well with the trends observed for temperature (Figure 10d) reflecting the temperature dependence of $NO_x$ formation reactions.

Note that the $\phi_m = 1.2$ exit plane profiles (Figure 11) intersect the $\phi_m = 1.0$ profiles with higher concentrations near the chamber wall. This is attributed to the additional production of $NO_x$ in the larger wake reaction zone associated with the rich mainstream. Although the recirculation zone

(b) $NO_x$ flow maps.

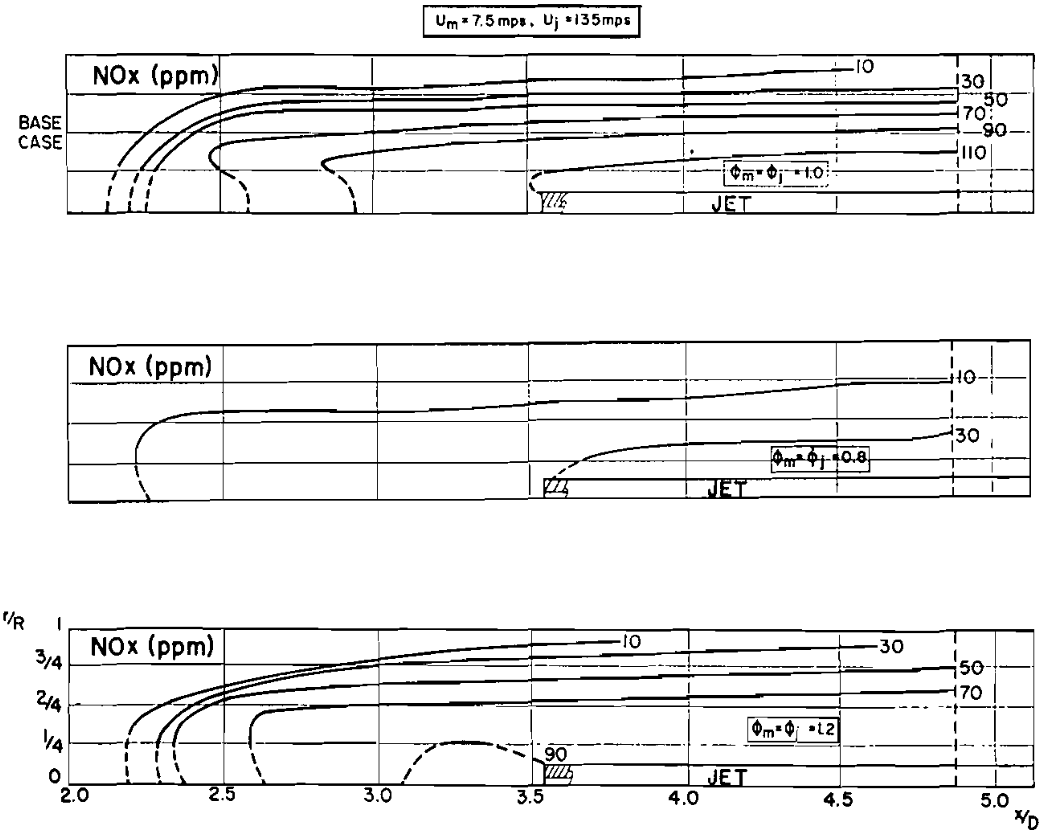


FIGURE 11 Parametric study: Effect of $\phi_m$ and $\phi_j$ ($NO_x$).

is larger as well, the data indicate that $NO_x$ production in the recirculation zone is not increased, a consequence of suppressed oxygen availability and temperature.

Jet equivalence ratio ($\phi_j$) directly impacts both the mixture ratio and temperature of the recirculation zone. As a result, the effect of jet equivalence ratio on $NO_x$ production is predictable. Production of $NO_x$ is increased with jet enrichment for lean mainstreams ($\phi_m = 0.6$, 0.8), decreased with jet enrichment or jet leaning for stoichiometric mainstream ($\phi_m = 1.0$), and increased with a lean jet or decreased with a rich jet for a rich ($\phi_m = 1.2$) mainstream.

The effect of mainstream equivalence ratio on the $NO/NO_x$ ratio is shown in Figure 12 for a stoichiometric jet. (Other jet equivalence ratios are omitted for clarity.) The rapid drop in the $NO/NO_x$ ratio occurs at the flame front for each of the cases ($\phi_m = 1.2$, 1.0, 0.8) wherein a wake reaction was supported. The low $NO/NO_x$ ratio for $\phi_m = 0.6$ is attributed to the quench zone surrounding the hot recirculation zone in the absence of a wake reaction.

## C. *Emission Indexes*

The emission indexes for $NO_x$, CO, and HC are presented in Figure 13 as a function of mainstream equivalence ratio ($\phi_m$). The parameters are jet equivalence ratio ($\phi_j$) and mainstream velocity ($U_m$). The procedure used to compute the emission index involved correcting the data for water vapor in the exhaust, calculating the area-averaged exit plane concentrations and the area-averaged mass emission, and taking the ratio of the mass emission to the fuel mass input.

The emission index data reflect the observations derived from the detailed results above, and place

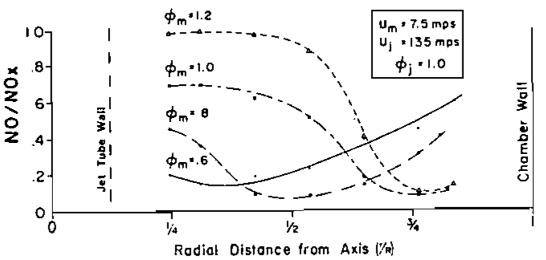


FIGURE 12 Parametric Study: Effect of $\phi_m$ ($NO/NO_x$).

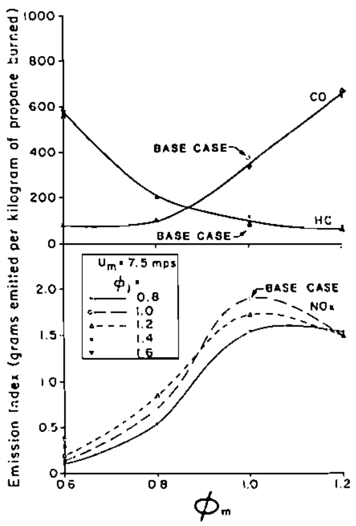


FIGURE 13 Emission indexes.

the performance of the combustor into a practical perspective. For example, $NO_x$ emissions are highest at $\phi_m = 1.0$, and are only slightly lower at 1.2. Values are 50 percent lower at $\phi_m = 0.8$ than at stoichiometric, and those at 0.6 are from 5 to 15 times lower than those for the base case (depending on jet equivalence ratio). The high temperatures that favor $NO_x$ formation also favor hydrocarbon oxidation. In the absence of a developed wake reaction at $\phi_m = 0.6$, 60 percent of the fuel is emitted unburned. As suggested by the analysis of the detailed flow maps, jet equivalence ratio has a minimum impact on HC and CO emission, but does affect $NO_x$ emission.

## SUMMARY

Aerodynamic flameholding is shown to provide control over pollutant formation and flame stability by direct, reactant injection into the recirculation zone. The data presented provide insight into the performance of the reverse jet flameholder, give guidance for practical application, and establish a data base for future testing of elliptic codes.

The reverse jet combustor, chemically and aerodynamically, consists of two distinct regions—the recirculation zone and the wake. The mainstream and jet velocity influence the size of these two regions, while the mainstream and jet mixture ratios affect the overall chemistry and heat release.

The influence of the jet on the emission of $NO_x$ is one of the more interesting characteristics of the flameholder. Jet changes which reduce the size, lower the temperature, and decrease the residence time are favorable to the reduction of $NO_x$ emission. For example, an enrichment of jet equivalence ratio affects recirculation zone temperature and mixture ratio, and will produce either an increase or decrease in the net emission of $NO_x$ depending on the mainstream equivalence ratio. Such changes do not significantly affect HC and CO emissions. A primary benefit from an enriched jet is to extend the lean blow-off limit and thereby maintain combustor stability simultaneous with a reduction in the emission of $NO_x$. However, a practical limit exists beyond which the emission of unburnt fuel is excessive. In the present experiment, this limit occurred at a mainstream equivalence ratio of approximately 0.8.


## ACKNOWLEDGEMENTS

This work was performed at the UCI Combustion Laboratory under sponsorship of the National Science Foundation, Grant No. ENG-7707797, and the Air Force Office of Scientific Research, Air Force Systems Command, USAF, Grant No. AFOSF 78-3586. Any opinions, findings, and conclusions or recommendations expressed in this publication are those of the authors and do not necessarily reflect the views of the National Science Foundation. The United States Government is authorized to reproduce and distribute reprints for Government purposes notwithstanding any copyright notations thereon. The contributions to the study by John T. Taylor (experimental facility design and operation) are gratefully acknowledged.


## REFERENCES


Anderson, S. J., Friedman, M. A., Krill, M. V., and Kesselring, J. P. (1981). Development of a Small-Scale Catalytic Gas Turbine Combustor, presented at the 1981 ASME International Gas Turbine Conference, ASME Paper 81-GT-43.

Chen, M. J., McLean, W. J., and Gouldin, F. C. (1979). The oxidation of NO to $NO_2$ during combustion quenching processes. Paper presented at the 1979 Spring meeting of the Western States Section/The Combustion Institute, WSS Paper No. 79–17, Brigham Young University, Provo, Utah, April.

Duclos, D. P., Schaffer, A. B., and Cambel, A. B. (1957). Flame-stabilizing effects of inclined air jets, *Industrial and Engineering Chemistry*, **49**, 2063.

Elghobashi, S. E., Samuelsen, G. S., Wuerer, J. E., and LaRue, J. C. (1981). Prediction and measurement of mass, heat and momentum transport in a nonreacting turbulent flow of a jet in an opposing stream, *Journal of Fluids Engineering*, **103**, 127.

Fristrom, R. M., and Westenburg, A. A. (1965). *Flame Structure*, McGraw-Hill, New York, p. 26.

McDannel, M. D. (1979). An experimental study of pollutant formation in premixed, propane–air fired, recirculating flow combustion, M.S. Thesis, Mechanical Engineering, University of California, Irvine, UCI Combustion Laboratory Report UCI-ARTR-79-1.

Oven, M. J., Gouldin, F. C., and McLean, W. J. (1979). Temperature and species concentration measurements in a swirl stabilized combustor. *Seventeenth Symposium (International) on Combustion*, The Combustion Institute, pp. 363–374.

Peck, R. E., and Samuelsen, G. S. (1977). Eddy viscosity modeling in the prediction of turbulent backmixed combustion performance. *Sixteenth Symposium (International) on Combustion*, The Combustion Institute, pp. 1675–1687.

Peterson, P. R., and Himes, R. M. (1978). Opposed jet combustor experimental facility, UCI Combustion Laboratory Report UCI-ARTR-78-8. Mechanical Engineering, University of California, Irvine.

Schaffer, A. B. (1954). Stabilizing effects of an opposing jet in high-velocity combustion, M.S. thesis, Northwestern University.

Schefer, R. W., and Sawyer, R. F. (1977). Lean premixed recirculating flow combustion for control of oxides of nitrogen. *Sixteenth Symposium (International) on Combustion*, The Combustion Institute, pp. 119–134.

Wuerer, J. E., and Samuelsen, G. S. (1979). Predictive modeling of backmixed combustor flows: mass and momentum transport, presented at the 17th AIAA Aerospace Sciences Meeting, New Orleans, AIAA Paper 79-0215.